Hybrid functional for correlated electrons in the projector augmented-wave formalism: Study of multiple minima for actinide oxides

F. Jollet, G. Jomard, and B. Amadon
CEA, DAM, DIF, F 91297 Arpajon, France

J. P. Crocombette and D. Torumba
SRMP, CEA-Saclay, 91191 Gif sur Yvette, France

(Received 19 June 2009; revised manuscript received 6 November 2009; published 3 December 2009)

Exact (Hartree-Fock) exchange for correlated electrons is implemented to describe correlated orbitals in the projector augmented-waves (PAW) framework, as suggested recently in another context [P. Novák *et al.*, Phys. Status Solidi B **243**, 563 (2006)]. Hartree-Fock exchange energy is applied to strongly correlated electrons only inside the PAW atomic spheres. This allows the use of PBE0 hybrid exchange-correlation functional for correlated electrons. This method is tested on NiO and results agree well with already published results and generalized gradient approximation, GGA+U calculations. It is then applied to plutonium oxides and UO_2 for which the results are comparable with the ones of GGA+U calculations but without adjustable parameter. As evidenced in the uranium oxide case, the occurrence of multiple energy minima may lead to very different results depending on the initial electronic configurations and on the symmetries taken into account in the calculation.

DOI: 10.1103/PhysRevB.80.235109 PACS number(s): 71.27.+a, 71.15.Mb

I. INTRODUCTION

Despite its impressive success, density-functional theory (DFT) applied in the frame of the local-density approximation (LDA) or generalized gradient approximation (GGA) fails to describe important properties of materials with correlated orbitals. Uranium dioxide, for instance, is found to be a metal, although it is experimentally established, it is a 2 eV gap insulator.[1] The same behavior is also found for plutonium oxides.[2,3] This failure is generally attributed to the fact that the exchange and correlation energy is too crudely treated in the frame of the LDA or GGA approximations. To overcome these difficulties, several methods have been proposed in the literature. A first attempt is the LDA+U method.[4–7] It leads to an orbital-dependent potential for the orbitals that are supposed to be localized, which corrects an aspect of the failure of the LDA approximation. Although it is possible to calculate the Hubbard parameter U, it is in practice considered as a parameter. The LDA+U method is a static approximation of the more general dynamical mean-field theory[8] that treats on site interactions thanks to many-body theory. This method is very promising, but for the moment, one need also to use a U parameter and the calculations are very time consuming. Another attempt is the self-interaction-corrected (SIC) (Ref. 9) LDA that removes the self-interactions of orbitals supposed to be localized. Interesting results have been obtained with this method but plane-wave implementations are scarse[10] and the calculations are also very time consuming.

A lot of work has also been devoted to new exchange-correlation functionals, and among them, to hybrid functionals[11] which combine Hartree-Fock (HF) exact exchange functionals with LDA or GGA functionals. They have shown to be very accurate for molecules (see, for instance, Ref. 12) without adjustable parameter. They have also been tested in solids (see Ref. 13 or the review[14]), but suffer from the high computational cost needed for the Fock integrals, in spite of some computational refinements.[15]

Recently, Novák *et al.* proposed to apply the exact exchange functional to a restricted subspace formed by the correlated electrons of a correlated system and called this method "exact exchange for correlated electrons" (EECE).[16] The implementation was done in a full-potential linearized augmented plane-wave (FPLAPW) code only inside the atomic spheres. It has then been adapted to perform hybrid-functional calculations restricted to specific electrons and applied to transition-metal monoxides[17] and to lanthanide and actinide impurities in Fe.[18] In each case, results are comparable or better than LDA+U calculations with the advantage of having no system-dependent parameter. Moreover these calculations should be much less computer time consuming than the full hybrid-functional method.

This last point is of great importance in view of testing hybrid functionals on very large systems, as, for example, defects in actinide compounds. Indeed, the large computational time needed for such calculations prevents the use of standard exact exchange approaches. That is why we want in this paper to test the possibility to perform EECE calculations on actinide systems with a computational time of the same order as standard DFT calculations. This implies to know whether the approximation made in the EECE frame is reasonable or not.

In this paper, the EECE approach is implemented in the projector augmented-waves (PAW) framework. The PBE0[19] exchange-correlation hybrid form functional is then applied for correlated orbitals only inside the PAW atomic spheres. This hybrid functional for correlated electrons (HFCE) is then tested on NiO, plutonium oxides, and UO_2.

In the first part of this paper, we review some aspects of the EECE formalism useful for this work. We give some details on our implementation within the PAW code ABINIT.[20–22] We then check that literature results[17] are repro-

duced within our implementation, taking NiO as an example. The second and main part is devoted to calculations on UO_2, PuO_2, and Pu_2O_3. We find that it is very difficult to obtain the correct ground state due to the occurrence of multiple local energy minima. Although already mentioned in literature for Hartree-Fock[23] or LDA+U (Refs. 24 and 25) calculations such occurrence of multiple minima is vastly overlooked. So we choose to present in some details the multiple energy minima accessible for bulk UO_2 and their dependence on the number of symmetries considered in the calculations.

II. HYBRID FUNCTIONAL FOR CORRELATED ELECTRONS METHOD IN PAW

In this section, we briefly review the hybrid functional for correlated electrons framework, its implementation within PAW, and we show some tests of our implementation.

A. Hybrid functional for correlated electrons method

We focus here on the PBE0[19] hybrid functional: in this frame the exchange-correlation energy is

$$E_{\mathrm{xc}}^{\mathrm{PBE0}}[\rho] = E_{\mathrm{xc}}^{\mathrm{PBE}}[\rho] + \frac{1}{4}(E_{\mathrm{x}}^{\mathrm{HF}}\{\Psi\} - E_{\mathrm{x}}^{\mathrm{PBE}}[\rho]), \tag{1}$$

where PBE refers to the Perdew-Burke-Ernzerhof GGA exchange-correlation functional.[26] Ψ and ρ represent the wave function and the corresponding electron density of the electrons, respectively.[17] The HF exchange term is

$$E_{\mathrm{x}}^{\mathrm{HF}}\{\Psi\} = -\frac{1}{2}\sum_{nn'}^{occ} \delta_{\sigma_n,\sigma_{n'}} \int d\vec{r}d\vec{r}' \frac{\Psi_n(\vec{r})\Psi_{n'}^*(\vec{r})\Psi_n^*(\vec{r}')\Psi_{n'}(\vec{r}')}{|\vec{r}-\vec{r}'|}, \tag{2}$$

where n and n' range over occupied states and σ_n and $\sigma_{n'}$ are the associated spins. As we are interested here only in localized correlated states due, for instance, to the d electrons of Ni in NiO or the f electrons of U in UO_2, we make the assumption that the correlated orbitals are zero outside the PAW sphere. This is similar to the assumptions made for the implementation of the LDA+U method in the PAW framework.[27,28] Following the notations of Ref. 27, the total wave function of the system inside the PAW sphere for a given state reduces to, if the partial-wave basis is complete

$$|\Psi_n\rangle = \sum_i \langle \tilde{p}_i|\tilde{\Psi}_n\rangle|\Phi_i\rangle, \tag{3}$$

where the index i stands for the atomic position $\vec{R}$, the angular momentum (l,m), and an additional index ν to label different partial waves for the same site and angular momentum. $\tilde{\Psi}_n$ are the pseudized wave functions. The Φ_i are the all-electron partial waves and $\tilde{p}_i$ are the projector functions.[29] Putting Eq. (3) into Eq. (2), and restricting the sums to the selected (sel) correlated orbitals, leads to

$$E_{\mathrm{x}}^{\mathrm{HF}}\{\Psi_{sel}\} = -\frac{1}{2}\sum_{\sigma}\sum_{ijkl}\int d\vec{r}d\vec{r}' \frac{\Phi_i(\vec{r})\Phi_j^*(\vec{r})\Phi_k^*(\vec{r}')\Phi_l(\vec{r}')}{|\vec{r}-\vec{r}'|}\rho_{i,k}^{\sigma}\rho_{j,l}^{\sigma} \tag{4}$$

with $\rho_{ij}^{\sigma} = \Sigma_{nk} f_{nk} \langle \tilde{\Psi}_{nk}^{\sigma}|\tilde{p}_i\rangle\langle\tilde{p}_j|\tilde{\Psi}_{nk}^{\sigma}\rangle$.

The partial wave functions are then separated between angular and radial parts

$$\Phi_i(\vec{r}) = \frac{\Phi_{\nu_i l_i}(r)}{r} S_{l_i m_i}(\hat{r}) \tag{5}$$

with $S_{lm}(\hat{r})$ the real spherical harmonics.

At the end, using the multipole expansion of the one-center Coulomb operator

$$E_{\mathrm{x}}^{\mathrm{HF}}\{\Psi_{sel}\} = -\frac{1}{2}\sum_{LM}\frac{4\pi}{2L+1}\sum_{\nu_i\nu_j\nu_k\nu_l} F_{\nu_i\nu_j\nu_k\nu_l}^{L} \times \sum_{m_i m_j m_k m_l}\langle m_i|LM|m_j\rangle\langle m_k|ML|m_l\rangle \sum_{\sigma}\rho_{m_i,m_k}^{\sigma}\rho_{m_j,m_l}^{\sigma}, \tag{6}$$

where $\langle m_i|LM|m_j\rangle$ are real Gaunt coefficients calculated for the selected l momentum and $F_{\nu_i\nu_j\nu_k\nu_l}^{L}$ are the Slater integrals.

$$F_{\nu_i\nu_j\nu_k\nu_l}^{L} = \int \frac{r_<^L}{r_>^{L+1}}\Phi_{\nu_i}(r)\Phi_{\nu_j}(r)\Phi_{\nu_k}(r')\Phi_{\nu_l}(r')drdr' \tag{7}$$

with $r_< = min(r,r')$ and $r_> = max(r,r')$. This result is equivalent to the formulation already established in Ref. 12 for the all-electron one-center part of the exchange energy. No spin-orbit coupling is taken into account in the calculations presented in this paper.

B. PAW implementation

The present results have been obtained within the PAW method as implemented in the ABINIT code.[20,22,27] It relies on an efficient fast Fourier transform (FFT) algorithm[30] for the conversion of wave functions between real and reciprocal space, on the adaptation to a fixed potential of the band-by-band conjugate-gradient method[31] and on a potential-based conjugate-gradient algorithm for the determination of the self-consistent potential.[32] The Slater integrals and the real Gaunt coefficients are calculated once and for all. From the knowledge of the occupation matrix ρ_{ij}^{σ}, the energy is calculated directly from Eq. (6) and from the quantity $E_{\mathrm{x}}^{\mathrm{PBE}}[\rho_{sel}]$. The HFCE Kohn Sham potential, computed following Blöchl[29] is deduced from the energy with $H^{\sigma} = \frac{dE}{d\tilde{\rho}^{\sigma}}$ with $\tilde{\rho}^{\sigma} = \Sigma_n |\tilde{\Psi}_n^{\sigma}\rangle f_n^{\sigma}\langle\tilde{\Psi}_n^{\sigma}|$ For $E_{\mathrm{HFCE}} = \frac{1}{4}(E_{\mathrm{x}}^{\mathrm{HF}}\{\Psi_{sel}\} - E_{\mathrm{x}}^{\mathrm{PBE}}[\rho_{sel}])$, it gives

$$H^{\sigma} = \frac{dE_{\mathrm{HFCE}}}{d\tilde{\rho}^{\sigma}} = \sum_{i,j}^{l_i=l_j=l_{\mathrm{HFCE}}} \underbrace{\frac{dE_{\mathrm{HFCE}}}{d\rho_{ij}^{\sigma}}}_{V_{m_i m_j}^{\mathrm{HFCE}}} \underbrace{\frac{d\rho_{ij}^{\sigma}}{d\tilde{\rho}^{\sigma}}}_{|\tilde{p}_i\rangle\langle\tilde{p}_j|} = \sum_{i,j}^{l_i=l_j=l_{\mathrm{HFCE}}} |\tilde{p}_i\rangle D_{ij}^{\mathrm{HFCE}}\langle\tilde{p}_j|. \tag{8}$$

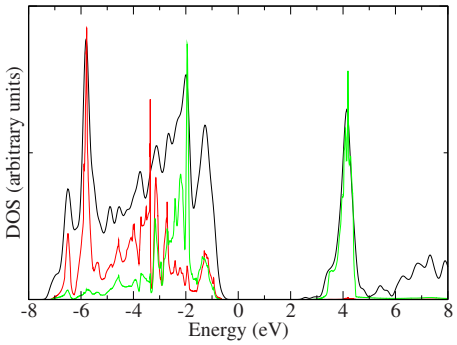

FIG. 1. (Color online) Projected d density of states of NiO in HFCE. The black curve is the total DOS; the dark and light gray (red and green online) curves are the partial $3d$ Ni spin-up and spin-down DOS.

l_{HFCE} is the angular momentum of the correlated orbitals ($l=2$ for d orbitals in Ni). We then have $D_{ij}^{\mathrm{HFCE}}=V_{m_i m_j}^{\mathrm{HFCE}}$, which is a contribution to the nonlocal part of the Hamiltonian. Derivating E_{HFCE} against ρ_{ij}^{σ} gives

$$V_{m_i m_j}^{\mathrm{HFCE}} = -\frac{1}{4}\sum_{LM}\frac{4\pi}{2L+1}\sum_{d_k d_l} F^{L}_{\nu_i\nu_j\nu_k\nu_l} \times \sum_{m_k m_l}\langle m_i|LM|m_k\rangle \times\langle m_j|ML|m_l\rangle \rho^{\sigma}_{m_k,m_l} - \frac{1}{4}\frac{dE_{\mathrm{x}}^{\mathrm{PBE}}[\rho_{sel}]}{d\rho_{ij}^{\sigma}}. \quad (9)$$

Note that as the HFCE energy depends explicitly on the cell parameters or the position of the atoms through the ρ_{ij}. Thus the only contribution to the forces or the stress is contained in the D_{ij}^{HFCE}. Note also that the validity of the HFCE approximation is closely related to the fact that the electronic density of the correlated orbitals are contained inside the PAW spheres. For the compounds studied in this paper, between 90% and 98% of this density is contained into the PAW spheres. This is of the same order as what is used within the LDA+U method.

C. Validation on nickel oxide

In order to validate our implementation, we show here some tests of our code on antiferromagnetic nickel oxide. LDA underestimates the gap and the magnetic moment in nickel oxide. They are better described in LDA+U.[4] In our calculation, $3s$ and $3p$ semicore states are treated in the valence for nickel. Valence states for oxygen are $2s$ and $2p$. The PAW matching radii are 2.3 and 1.91 a.u. for nickel and oxygen. The energy cutoff for the plane-wave expansion of the pseudowave function is 24 Ha. In this case, the variation in the spin moment is less than 0.1%. The energy is converged within less than 0.5 mHa. 63 k points are used in the irreducible Brillouin zone. 97.5% of the d atomic wave function is contained inside the augmentation region, which validates the assumption that the HFCE method be applied inside the PAW sphere only.

Our total and projected calculated density of states (DOS) are shown on Fig. 1. These DOS are physically sound. Moreover present HFCE results are very close to the calculation of Tran *et al.*,[17] that are made with the same method in a FPLAPW context. Our lattice constant, bulk modulus, and magnetic moment are the nearly identical to theirs (see Table I).

TABLE I. Lattice parameter, bulk modulus, magnetic moment, and gap for NiO in the PAW-HFCE frame compared to FPLAPW-HFCE calculations and to experiment.

	Expt.[a]	PAW-HFCE	FPLAPW-HFCE[b]
a (Å)	4.17	4.23	4.24
B (GPa)	166–208	185.6	187
μ_s (μB)	1.64–1.90	1.75	1.73
Gap (eV)	4.0–4.3	2.8	2.8

[a]References 33–37.
[b]Reference 17.

The value of the gap obtained from our calculation is 2.8 eV. We see that our values for the gap and the spin moment are in the range of existing LDA+U implementations,[24] including FLAPW calculations. Our results are within 0.1 eV independent of the choice of the PAW matching radius.

III. RESULTS AND DISCUSSION

A. Occurrence of metastable states

In this section, we underline the need for a careful search of the ground state of a correlated system with hybrid functionals. The occurrence of metastable states is peculiar to methods which localize electrons: It has for long been emphasized in Hartree-Fock calculations (see, e.g., Ref. 23), and also appears with LDA+U (Refs. 24 and 25) or SIC.[9] It is due to the fact that these methods introduce an orbital anisotropy: filled orbitals are energetically favored over empty ones. A lots of minima thus appear: they correspond to different initial (i.e., prior to applying LDA+U or HFCE) occupations of orbitals by the electrons. In LDA+U, as well as in HFCE (see below the UO_2 case), as the difference of energies between orbitals are weak compared to the electron-electron interaction, these minima are close in energy.[28] In order to find the ground state, the energies of these minima have to be compared. A way to find the ground state of a correlated insulating system in LDA+U has been described in Ref. 3. In the HFCE scheme, a similar method has been used: at the beginning of a given calculation, a given ρ_{ij} has been imposed to the system in order to stabilize the corresponding electronic configuration. Whereas in NiO, the ground state is obvious to find in term of occupations of d orbitals, it is not the case in UO_2 where f orbitals are closer in energy. Note also that the calculations presented in this paper do not include the spin-orbit coupling. The inclusion of spin-orbit coupling would change completely the energetics of the multiple minima. The following analysis should therefore be done again (especially the m quantum number would no more be a good quantum number).

B. Calculations on plutonium oxides

In a recent paper, we studied structural, thermodynamic, and electronic properties of plutonium oxides from first prin-

TABLE II. Equilibrium properties of PuO_2 and Pu_2O_3. Structural parameters (V_0 and B_0) as well as band-gap energy (Δ) and total-energy differences ($E_{FM}-E_{AFM}$) are reported. We compare the results obtained within the GGA+U (U=4.0 eV and J=0.7 eV) framework with the ones obtained using the HFCE-PBE0 hybrid functional. Both sets of data are compared with experiments and with the results of Prodan *et al.* (Ref. 2) that uses full hybrid functional.

Compound	Method	Magnetism	V_0 (Å^3)	B_0 (GPa)	Δ (eV)	$E_{FM}-E_{AFM}$ (meV)
PuO_2	PBE+U	AFM	40.34	199	2.2	14
	$PBE0_{HFCE}$	AFM	39.91	202	2.1	45
	$PBE0_{full}$ [a]	AFM	39.04	221	3.4	14
	HSE[a]	AFM	39.28	220	2.6	14
	Expt.		39.32[c]	178[d]	1.8[e]	
Pu_2O_3	PBE+U	AFM	78.08	110	1.7	4
	$PBE0_{HFCE}$	AFM	77.09	139	1.5	22
	Expt.[b]		75.49–76.12		>0	>0

[a]Reference 2.
[b]References 39 and 40.
[c]Reference 41.
[d]Reference 42.
[e]Reference 43.

ciples within the GGA+U framework.[3] In the following, we show that our HFCE implementation of the PBE0 hybrid functional allows to recover our GGA+U results for both PuO_2 and β-Pu_2O_3 compounds without tuning any adjustable parameter.

The computational details of the present calculations (PAW atomic data, energy cutoffs, k-point sampling,…) are the same as the ones used in our previous work.[3] In order to find the true ground state among the various metastable solutions that appear with hybrid functionals, we performed a large number of calculations starting from the density matrices that correspond to all the possible ways of distributing the f electrons of plutonium among the seven m orbitals available. For PuO_2, plutonium atoms carry four f electrons in a completely ionic solution while in Pu_2O_3 this number is raised to five. Consequently, we have tested, respectively, 35 and 21 guesses for the initial density matrices (we have considered only integer occupations of the m orbitals). In the case of the sesquioxide we found the same ground state within the LDA/GGA+U and HFCE-PBE0 frameworks. For PuO_2 it appears that the ground state found using the HFCE-PBE0 is different from the one obtained with the LDA/GGA+U method. If we use the notation of Refs 28 and 38 for the f orbitals, the HFCE-PBE0 ground state corresponds to the filling of the two doubly degenerated E_u levels.

In Tables II and III we gather the results of our present PBE0 calculations as well as the ones taken from our previous LDA/GGA+U work.[3] Note that as concerns the β-Pu_2O_3 compound we perform a complete structural relaxation of the β-Pu_2O_3 compound (these results are given in Table II). We also consider the experimental geometry of this compound by fixing the c/a ratio and the internal parameters to their experimental values in order to compare our results to the ones of Prodan and co-workers who work in these conditions (these results are given in Table III). As concerns the structural parameters and the band-gap energies, the agreement between HFCE-PBE0 and GGA+U calculations is better than 5%. Like the GGA+U framework, the HFCE-PBE0 allows to recover a proper insulating behavior for both plutonium oxides with band-gap energies close to the available experimental data. We find that equilibrium volumes obtained with HFCE-PBE0 are closer to experiments than the ones calculated within the GGA+U framework, which is in agreement with a full PBE0 calculation by Prodan *et al.*[2] Both HFCE-PBE0 and GGA+U calculations agree with an antiferromagnetic (AFM) ground state for PuO_2 and Pu_2O_3 compounds. However the use of a PBE0 hybrid functional greatly promotes this state compare to the ferromagnetic one. The comparison of the electronic DOS calculated within the HFCE-PBE0 and GGA+U frameworks (see Fig. 2) reveals strong differences for both PuO_2 and Pu_2O_3. First, as concerns the plutonium dioxide, the use of HFCE-PBE0 tends to shift the Pu 5f states upwards in energy in the valence band compared to what is obtained within the GGA+U frame-

TABLE III. Equilibrium properties of β-Pu_2O_3 for a fixed lattice-parameter ratio a_0/c_0=0.64468 which corresponds to the experimental measurment by Flotow and Tetenbaum (Ref. 44). Structural parameters a_0, B_0 as well as the band-gap energy (Δ) or magnetic properties (corresponding to the total-energy differences $E_{FM}-E_{AFM}$) are reported. DFT+U calculations are performed with the following set of parameters, U=4.0 eV and J=0.7 eV.

Method	a_0 (Å)	B_0 (GPa)	Δ (eV)	$E_{FM}-E_{AFM}$ (meV)
PBE+U	3.879	137	1.65	3
$PBE0_{HFCE}$	3.857	139	1.5	21
$PBE0_{full}$ [a]	3.824	175	3.50	11
HSE[a]	3.822	158	2.78	3

[a]Reference 2.

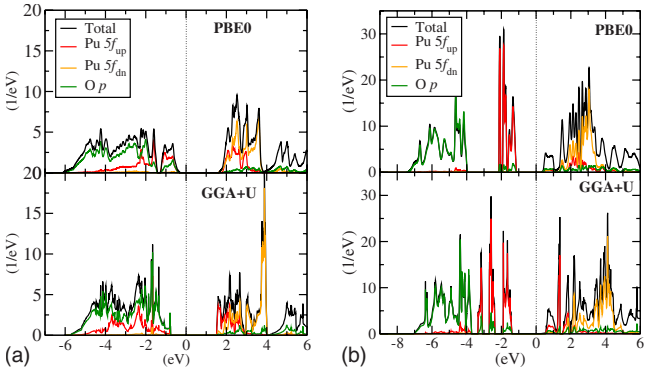

FIG. 2. (Color online) (a) Total and projected density of states of PuO_2 and (b) Pu_2O_3 computed for the ground states in the HFCE-PBE0 and GGA+U frameworks.

work. At the same time, the O $2p$ states are nearly unchanged. The differences are even larger for the Pu_2O_3 oxide since the DOS calculated within the GGA+U method clearly exhibits three distinct $5f$ peaks that span from −1.5 down to −3.5 eV. Whereas on the HFCE-PBE0 DOS, these peaks are very close to each other and thus only spread over an energy range going from −1.1 down to −2.1 eV. The lower part of the conducting band is also different since GGA+U calculations lead to the presence of a Pu $5f$ peak at around 1 eV that does not exist in the HFCE-PBE0 DOS.

Our HFCE-PBE0 DOSs are very similar to the ones published by Prodan *et al.*[2] with full hybrid functional. The main difference is that the latter predict much larger energy gaps than us. For PuO_2, their values are 1.5 times ours and this ratio reaches 2.3 for Pu_2O_3. We believe that this can be explained by the fact that in our calculations, only the part of the f orbitals of the plutonium atoms that located inside the PAW spheres are treated with the PBE0 hybrid functional whereas in the approach of Prodan and co-workers all electrons are treated at the PBE0 level. Another point to focus on is the fact that short-range hybrid functionals, as the HSE one, are known to be more accurate to reproduce gaps than the PBE0 one. When comparing to the HSE results of Prodan *et al.*,[2] the gaps we have calculated (Tables II and III) are closer to the HSE ones rather than to the PBE0 ones. An explanation could be that, as the HFCE is restricted into the PAW spheres, it is in a crude way a more or less short-range functional.

C. Calculations on bulk uranium dioxide

The suitable PAW atomic data for uranium and oxygen atoms were generated using the ATOMPAW tool.[45] The cutoff energy used for all the calculations is 35 Ha while the energy cutoff for the fine FFT grid was set to 40 Ha. The conventional cell of UO_2, containing 12 atoms (fluorite structure, space group $Fm3m$), was taken as unit cell which allowed us to consider the collinear $1-k$ antiferromagnetic structure to be studied. In this structure, planes of alternate spins are ordered along a 100 plane which reduces the number of point-group symmetries in the structure from 48 to 16. However, the unit cell being nonprimitive, there are nonsymmorphic symmetries to take into account, which leads to a total of 64 symmetries.

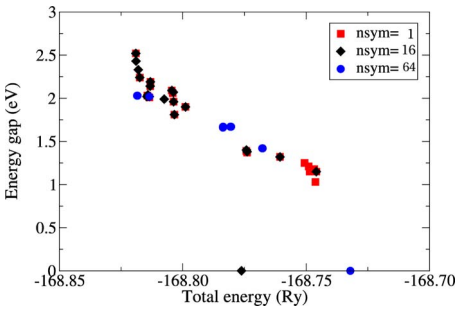

FIG. 3. (Color online) The energy band gap as a function of the total energy (per formula unit of UO_2) for the solutions obtained using a different number of symmetry operations: nsym=1 (squares), nsym=16 (diamonds), and nsym=64 (circles).

As underlined above, metastable solutions appear with hybrid functionals depending on the starting point of the calculations. We have performed calculations corresponding to all the possible ways of distributing the two f electrons of uranium over the seven m (up) orbitals, as has been done in Ref. 46. Considering only integer occupation of the m orbitals, one ends up with 21 possible combinations. In these calculations the corresponding ρ_{ij} term was kept fixed for the first 30 self-consistent iterations. Due to the application to the wave functions of the 64 symmetry operations acting in the perfect fluorite structure one ends up with six different mestastable solutions (see Fig. 3) which exhibit various energies and band gaps.

However, it has been shown that for localized f orbitals it might be necessary to break the crystal symmetry[25] in order to get to the correct ground state. Indeed a localized f orbital might have a lower symmetry than the crystal imposes, and if the symmetry constraint is not lifted this orbital cannot be properly occupied. Therefore, we performed two additionally sets of calculations. In the first set no symmetry beyond identity was considered (nsym=1 in Fig. 3). One then obtains 21 different solutions. In the second intermediate set only 16 symmetry operations are considered: this corresponds to the symmetries that remain when a small displacement of the O atoms from the ideal positions perpendicular to the direction of magnetization is introduced (see below the discussion of the Jahn-Teller effect). This intermediate case leads to 17 different metastable states. The total energies obtained with these three symmetry sets are plotted in Fig. 3 together with the corresponding band gap. For these calculations we used a $2\times2\times2$ **k**-point grid, which yielded 1 or 2 or 4 special **k** points in the irreducible part of the BZ, depending on the number of the symmetry operations considered (64, 16, and 1, respectively).

Two points are worth noting in view of this figure. First, the starting point of the calculations does indeed affect a lot the outcome of the calculations. One observes huge variations in the total energies and of the band gaps. The latter can even be zero for some starting configurations. Second, the solutions that have lower energies tend to have larger band gaps. For nsym=1 and nsym=16 the ground-state solution is identical, having a band gap of 2.52 eV, while for nsym

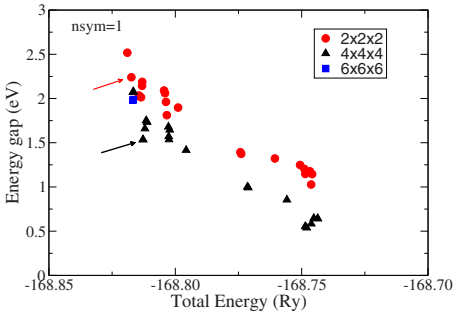

FIG. 4. (Color online) The energy band gap as a function of the total energy (per formula unit of UO_2) for the solutions obtained using a different k mesh: $2\times2\times2$ (red balls), $4\times4\times4$ (black triangles), and $6\times6\times6$ (blue squares). Red and black arrows point to the solutions obtained starting from the Jahn-Teller distorted spin-GGA calculation with $2\times2\times2$ and $4\times4\times4$ k meshes.

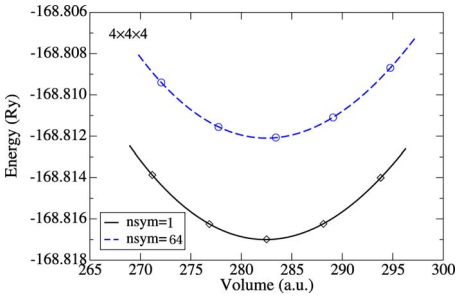

FIG. 5. (Color online) Variation in the total energy (per formula unit) of the lowest energy solutions of UO_2 obtained for nsym=1 (solid black line) and nsym=64 (dashed blue line), using a $4\times4\times4$ k mesh. The lines represent the Birch-Murnaghan fit through the calculated points.

=64 we get a different ground-state solution, slightly higher in energy, with a gap of 2.03 eV. The lowest energy obtained when using nsym=1 and nsym=16 corresponds to the $m=-3$ and $m=0$ orbitals occupied while for nsym=64 the two f electrons occupy the $m=-3$ and $m=-1$ orbitals. It is clear that without lowering the symmetry one does not have access to the lowest-energy solution obtained with nsym=1 (or nsym=16).

Subsequently, for the case of nsym=1 we increased the k mesh to $4\times4\times4$ and for the two solutions that have the lowest energies to $6\times6\times6$. All these additional calculations were fully converged to self-consistency. As can be seen in Fig. 4, although the energy does not change much when going to the $4\times4\times4$ k mesh, the change in the width of the band gap is significant. In this way, for the lowest-energy solution the band gap decreases from 2.52 to 2.07 eV for a $4\times4\times4$ k mesh and 1.98 eV for a $6\times6\times6$ k mesh. For the finest k mesh the two lowest-energy solutions ($m=-3$ and $m=0$ orbitals occupied and $m=+3$ and $m=0$ occupied) become almost indistinguishable (see Fig. 4).

One thus ends up with many different solutions depending on the starting points of the calculations and on the considered symmetries. As indicated above, this relates to the fact that hybrid functional (as well as LDA+U calculations) tend to strongly separate occupied states from empty states. Once separated, they can no longer mix. Occupied f states in a given configuration at the beginning of the calculations are so favored by the application of the hybrid functional that they will never empty. And so the calculation converges to the lowest energy with this f state configuration even if another occupation would give a lower energy. We have above used what could be defined as a "brute force" method to find the ground state: namely, testing as many as possible starting points and sorting the many obtained results. It would of course be more satisfactory to determine beforehand what the lowest-energy configuration will be. This comes down to pre-establish what the occupation matrix of f orbitals should be. Unfortunatly it is only possible to make guesses about what such configuration. The best guessing method we found is based on the existence of Jahn-Teller (J-T) distortion in UO_2.[47] Considering this distortion in a spin-GGA (PBE) calculation, one obtains an occupation matrix for f orbitals that can be assumed to be the one of the true ground state. To check this assumption we slightly shifted the oxygen positions according to the J-T distortion, then performed a spin-polarized GGA calculation without hybrid functional. One obtains a GGA ground state which is essentially metallic but with a very small energy separation between occupied and empty f states. We then turned on the hybrid functional starting from the spin-GGA wave functions. We also relaxed the oxygen positions to measure the amount of J-T distortion. This calculation was done considering all symmetries present with the atomic displacements, i.e., with the 16 symmetries of the aforementioned nsym=16 case. We found that the finally obtained distortion after relaxation is completely negligible, the oxygen atoms moving back to their perfect positions. Moreover the obtained result proves to be one of those obtained from the various starting points of the previous series of calculations. Indeed for a $2\times2\times2$ k mesh one eventually obtains $m=0$ and $m=+3$ orbitals occupied while for a $4\times4\times4$ k mesh one has $m=+1$ and $m=+3$ orbitals occupied.

These states are not the ones of lowest energy for the corresponding k meshes. Our guess procedure is therefore not working perfectly. However, it leads to states which are very close to the "true" ground states calculated with the systematic procedure with a difference in energy lower than 10^{-2} Ha/f.u.. Such guess procedure may therefore be of interest when the systematic search of the exact density matrix of the f electrons is not feasible.

We now come back to the ground states obtained with the systematic search using the full symmetry (nsym=64) or the lowered symmetry (nsym=1) and describe the properties of these ground states. The variation in total energy with volume is given in Fig. 5 for both solutions. As it can be seen the shape of the corresponding Birch-Murnaghan fits are very similar, yielding the same equilibrium volume and the same bulk modulus (see also Table IV). The calculated equilibrium properties of the two lowest-energy solutions obtained with nsym=1 and nsym=64 are compared with the ones obtained using different functionals and with experiment in Table IV. As it can be observed, using the HFCE-PBE0 functional one can get a nice agreement with experiment, comparable in quality to the GGA+U method. For which concerns the values of the gaps, the same conclusion

TABLE IV. Comparison of the calculated equilibrium lattice constant (a_0), bulk modulus (B_0), and the band gap (ΔE) of UO_2 using different energy functionals and experiment.

	a_0 (a.u.)	B_0 (GPa)	ΔE (eV)
$PBE0_{HFCE}$(nsym=1)	10.416	199	1.98
$PBE0_{HFCE}$(nsym=64)	10.415	199	1.66
$PBE0_{full}$ [a]	10.307	219	3.13
HSE[a]	10.324	218	2.39
LDA[b]	9.902	252	0
LDA+U [c]	10.431	209	1.80
Expt.[d]	10.343	207	2.10

[a]Reference 2.
[b]Reference 48.
[c]Reference 49.
[d]References 42 and 50.

as for plutonium oxides can be done when comparing to the PBE0 and HSE ones.

By comparing the DOS plot of the two solutions (Fig. 6) we can see that they are very similar too. The only significant difference is the width of the peaks near the Fermi level, which results in a difference in the band gap. The general shape of DOS is similar to the one obtained using the full version of the PBE0 functional.[2]

IV. CONCLUSION

We have implemented the hybrid functional for correlated electrons formalism of Novák *et al.* in the ABINIT code within PAW formalism. Satisfactory results are obtained for plutonium and uranium oxides. Such an implementation of the PBE0 hybrid-functional framework is therefore able to capture the main physical properties of strongly correlated systems. The level of description is on the same order of the one provided by the GGA+U framework without the need to adjust the U parameter while such implementation of the PBE0 hybrid functional is much less computational consuming than the standard one. This opens the way to use in this framework big unit-cell calculations that are necessary to study, for instance, the influence of defects on the properties of correlated oxides.

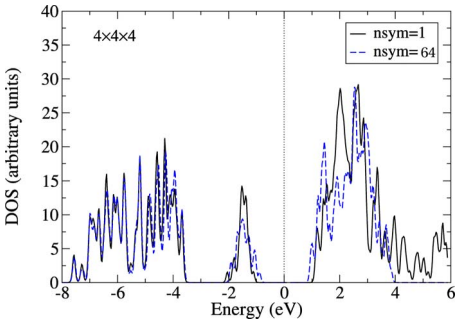

FIG. 6. (Color online) Total DOS of UO_2.

The occurrence of multiple energy minima depending on the initial occupation of the correlated orbitals that appears in GGA+U or standard hybrid functional also shows up in the present implementation of hybrid functionals. As evidenced in the uranium oxide case, one may obtain very different results depending on the initial electronic configurations and on the symmetries taken into account in the calculation. For the specific case of UO_2 we exhibited a procedure which allows to obtain a quite satisfactory guess of the true ground state without the need to systematically search all the possible density matrices of the f electrons.

ACKNOWLEDGMENTS

We would like to thank Marc Torrent for fruitful discussions and Andres Saul (CINAP, Aix-Marseille) for suggesting the guess procedure for the search of the ground state of UO_2.

[1] S. L. Dudarev, D. Nguyen Manh, and A. P. Sutton, Philos. Mag. B **75**, 613 (1997).
[2] I. D. Prodan, G. E. Scuseria, and R. L. Martin, Phys. Rev. B **73**, 045104 (2006).
[3] G. Jomard, B. Amadon, F. Bottin, and M. Torrent, Phys. Rev. B **78**, 075125 (2008).
[4] V. I. Anisimov, J. Zaanen, and O. K. Andersen, Phys. Rev. B **44**, 943 (1991).
[5] V. I. Anisimov, F. Aryasetiawan, and A. I. Lichtenstein, J. Phys.: Condens. Matter **9**, 767 (1997).
[6] A. I. Liechtenstein, V. I. Anisimov, and J. Zaanen, Phys. Rev. B **52**, R5467 (1995).
[7] M. T. Czyżyk and G. A. Sawatzky, Phys. Rev. B **49**, 14211 (1994).
[8] A. Georges, G. Kotliar, W. Krauth, and M. J. Rozenberg, Rev. Mod. Phys. **68**, 13 (1996).
[9] M. Lüders, A. Ernst, M. Dane, Z. Szotek, A. Svane, D. Kodderitzsch, W. Hergert, B. L. Gyorffy, and W. M. Temmerman, Phys. Rev. B **71**, 205109 (2005).
[10] M. Stengel and N. A. Spaldin, Phys. Rev. B **77**, 155106 (2008).
[11] A. D. Becke, J. Chem. Phys. **98**, 5648 (1993).
[12] J. Paier, R. Hirschl, M. Marsman, and G. Kresse, J. Chem. Phys. **122**, 234102 (2005).
[13] K. N. Kudin, G. E. Scuseria, and R. L. Martin, Phys. Rev. Lett. **89**, 266402 (2002).
[14] F. Corà, M. Alfredsson, G. Mallia, D. S. Middlemiss, W. C. Mackrodt, R. Dovesi, and R. Orlando, *Structure and Bonding* (Springer-Verlag, Berlin, 2004).
[15] M. Marsman, J. Paier, A. Stroppa, and G. Kresse, J. Phys.: Condens. Matter **20**, 064201 (2008).
[16] P. Novák, J. Kunes, L. Chaput, and W. E. Pickett, Phys. Status Solidi B **243**, 563 (2006).
[17] F. Tran, P. Blaha, K. Schwarz, and P. Novák, Phys. Rev. B **74**, 155108 (2006).

[18] D. Torumba, P. Novák, and S. Cottenier, Phys. Rev. B **77**, 155101 (2008).
[19] M. Ernzerhof and G. E. Scuseria, J. Chem. Phys. **110**, 5029 (1999).
[20] X. Gonze, J.-M. Beuken, R. Caracas, F. Detraux, M. Fuchs, G.-M. Rignanese, L. Sindic, M. Verstraete, G. Zerah, F. Jollet, M. Torrent, A. Roy, M. Mikami, Ph. Ghosez, J.-Y. Raty, and D. C. Allan, Comput. Mater. Sci. **25**, 478 (2002).
[21] X. Gonze *et al.*, Z. Kristallogr. **220**, 558 (2005).
[22] The ABINIT code is a common project of the Université Catholique de Louvain, Corning Incorporated, the Université de Liège, the Commissariat à l'Energie Atomique, Mitsubishi Chemical Corp., the Ecole Polytechnique Palaiseau, and other contributors, http://www.abinit.org
[23] H. Fukutome, Prog. Theor. Phys. **45**, 1382 (1971).
[24] A. B. Shick, A. I. Liechtenstein, and W. E. Pickett, Phys. Rev. B **60**, 10763 (1999).
[25] P. Larson, W. R. L. Lambrecht, A. Chantis, and M. van Schilfgaarde, Phys. Rev. B **75**, 045114 (2007).
[26] J. P. Perdew, K. Burke, and M. Ernzerhof, Phys. Rev. Lett. **77**, 3865 (1996).
[27] M. Torrent, F. Jollet, F. Bottin, G. Zérah, and X. Gonze, Comput. Mater. Sci. **42**, 337 (2008).
[28] B. Amadon, F. Jollet, and M. Torrent, Phys. Rev. B **77**, 155104 (2008).
[29] P. E. Blöchl, Phys. Rev. B **50**, 17953 (1994).
[30] S. Goedecker, SIAM J. Sci. Comput. (USA) **18**, 1605 (1997).
[31] M. C. Payne, M. P. Teter, D. C. Allan, T. A. Arias, and J. D. Joannopoulos, Rev. Mod. Phys. **64**, 1045 (1992).
[32] X. Gonze, Phys. Rev. B **54**, 4383 (1996).
[33] A. K. Cheetham and D. A. O. Hope, Phys. Rev. B **27**, 6964 (1983).
[34] H. A. Alperin, J. Phys. Soc. Jpn. **17-B3**, 12 (1962).
[35] W. Neubeck, C. Vettier, V. Fernandez, F. de Bergevin, and C. Giles, J. Appl. Phys. **85**, 4847 (1999).
[36] G. A. Sawatzky and J. W. Allen, Phys. Rev. Lett. **53**, 2339 (1984).
[37] S. Hüfner, J. Osterwalder, T. Riesterer, and F. Hulliger, Solid State Commun. **52**, 793 (1984).
[38] M. Blanco, M. Flórez, and M. Bermejo, J. Mol. Struct.: THEOCHEM **419**, 19 (1997).
[39] B. McCart, G. Lander, and A. Aldred, J. Chem. Phys. **74**, 5263 (1981).
[40] M. Wulff and G. Lander, J. Chem. Phys. **89**, 3295 (1988).
[41] J. Haschke, T. Allen, and L. Morales, Science **287**, 285 (2000).
[42] M. Idiri, T. LeBihan, S. Heathman, and J. Rebizant, Phys. Rev. B **70**, 014113 (2004).
[43] C. McNeilly, J. Nucl. Mater. **11**, 53 (1964).
[44] H. Flotow and M. Tetenbaum, J. Chem. Phys. **74**, 5269 (1981).
[45] N. A. W. Holzwarth, A. R. Tackett, and G. E. Matthews, Comput. Phys. Commun. **135**, 329 (2001).
[46] B. Dorado, B. Amadon, M. Freyss, and M. Bertolus, Phys. Rev. B **79**, 235125 (2009).
[47] R. Caciuffo, G. Amoretti, P. Santini, G. H. Lander, J. Kulda, and P. deV. DuPlessis, Phys. Rev. B **59**, 13892 (1999).
[48] J. P. Crocombette, F. Jollet, L. T. Nga, and T. Petit, Phys. Rev. B **64**, 104107 (2001).
[49] F. Gupta, G. Brillant, and A. Pasturel, Philos. Mag. **87**, 2561 (2007).
[50] J. Schoenes, J. Appl. Phys. **49**, 1463 (1978).